On the Nature of the Diffraction Figures due to the Heliometer.

By Philip Francis Everitt, University College, London.

(Communicated by Prof. Karl Pearson, F.R.S.—Received September 11,—Read November 25, 1909.)

[Plate 3.]

1. In investigating the influence of personal equation in connection with double star measurements, the actual values of distance and position angle must be known, and hence the only possible method is to use an artificial star. The method adopted in the Students' Observatory at University College, in order to obtain a known separation and direction, is to use a weak heliometer lens in front of the equatorial and a spark between cadmium electrodes some distance away. The direction of the line joining the two "star" images and the distance between them can be measured by a divided circle and micrometer screw respectively, while the intensity of the stars can be altered by using various stops. It was found that when a moderately small stop was used, the diffraction images became quite perceptible, and hence, before any further progress could be made in the determination of personal equation, it was necessary to investigate these diffraction images.

2. On consulting the literature of the subject, I found that the earliest papers dealing with the diffraction figure of the heliometer are by Bessel. He observed (*a*) that two opposite brushes of light emerged from the central disc perpendicularly to the line of separation; (*b*) that when the halves of the lens were separated, the disc was lengthened in the direction perpendicular to the line of separation; and (*c*) that the brushes of light were of equal length when the halves were united; but that, when the halves were separated, the brush of light on the same side of the image as the half-lens forming it was longer than the one on the opposite side; and he attributed the lengthening of the disc formed by the half-lens to the fact that the lens was corrected for spherical aberration for the whole lens, and not for the two halves separately.

This explanation does not, I think, require further examination. He also observed that there was an instability of superposition of the two images, and this was confirmed by Hansen and Gauss. In 1882 Bruns treated the diffraction figure of the semicircular aperture analytically, and gave formulæ for the intensity of the light at any point. These formulæ demand, however, a very large amount of arithmetical work before they can be of practical use. Bruns stated further that the task of computing the distribution of

light in the image had been undertaken by Schnauder. The only other paper on the subject was by Scheiner and Hirayama. It consisted chiefly of plates of photographs of diffraction images formed by various apertures, including the semicircle, and a brief summary of the paper by Bruns already mentioned. There are also notes and a definite statement that the calculations initiated by Prof. Bruns had not been completed.

3. I decided to attack anew the problem of computing the diffraction figure, hoping by the help of modern mechanical integrators to be more successful. The formulæ developed by Bruns give the light intensity, H, in terms of two components C and S, such that

$$H = C^2 + S^2,$$

where

$$C = \pi\gamma^2 \frac{J_1(\delta)}{\delta}, \qquad S = 2\gamma^2 \int_0^\epsilon \frac{1}{v}\left(\frac{\sin v}{v} - \cos v\right) du, \quad \text{and} \quad v = \delta \cos u;$$

δ and ϵ being the ray and angle polar co-ordinates of any point of the diffraction image referred to the centre of the image as pole, and a line parallel to the diameter of the aperture as initial line, and γ, a constant such that, if the intensity at the centre of the image be taken as unity, we must put $\pi\gamma^2 = 2$.

The values of C are obtained without difficulty from any table of Bessel functions for a somewhat limited range of values of δ, but the values of S depend on the evaluation of the integral $I = \int_0^\epsilon \frac{1}{v}\left(\frac{\sin v}{v} - \cos v\right) du$.

Three methods suggest themselves, namely (1) to make this integral depend on other tabulated integrals, (2) to expand in series, and (3) to evaluate by mechanical integration. It was not found possible to use the first method, and so only methods (2) and (3) were available. Since $v = \delta \cos u$, it is clear that the choice of method depends largely upon the range of values of δ that are to be considered. Now δ in the portion of the diffraction figure actually drawn ranges from 0 to 16·47. For the central region from 0 to 3·83 expansion by Taylor's theorem was used, and for the remaining portion, where expansions of the integral converged with extreme slowness, mechanical integration was adopted.

4. Evaluation by expansion, using Taylor's theorem. With the usual notation, let $f(0)$ be the value of the function I and $f^n(0)$ the value of the nth derived function when δ is put equal to 0 after obtaining the derived function.

Let

$$I = \int_0^\epsilon \frac{1}{v}\left(\frac{\sin v}{v} - \cos v\right) du,$$

then $$I = \int_0^\epsilon \frac{\sin v}{v^2}\,du - \int_0^\epsilon \frac{\cos v}{v}\,du$$

$$I = \int_0^\epsilon \frac{\sin(\delta\cos u)\,du}{\delta^2\cos^2 u} - \int_0^\epsilon \frac{\cos(\delta\cos u)\,du}{\delta\cos u};$$

$$\therefore\quad I\delta^2 = \int_0^\epsilon \frac{\sin(\delta\cos u)\,du}{\cos^2 u} - \int_0^\epsilon \frac{\delta\cos(\delta\cos u)\,du}{\cos u};$$

$$\frac{d}{d\delta}(I\delta^2) = \int_0^\epsilon \frac{\cos'(\delta\cos u)\,du}{\cos u} - \int_0^\epsilon \frac{\cos''(\delta\cos u)\,du}{\cos u} + \int_0^\epsilon \delta\sin(\delta\cos u)\,du,$$

or $$\delta\frac{dI}{d\delta} + 2I = \int_0^\epsilon \sin(\delta\cos u)\,du; \qquad \therefore\ f(0) = 0.$$

Differentiating again,

$$3\,\frac{dI}{d\delta} + \delta\frac{d^2I}{d\delta^2} = \int_0^\epsilon \cos(\delta\cos u)\cos u\,du; \qquad \therefore\ f'(0) = \tfrac{1}{3}\int_0^\epsilon \cos u\,du.$$

Proceeding, $$4\frac{d^2I}{d\delta^2} + \delta\frac{d^3I}{d\delta^3} = -\int_0^\epsilon \cos^2 u\sin(\delta\cos u)\,du,$$

whence $$f''(0) = 0.$$

As we proceed further we shall always, in the case of the derived functions of even order, have on the right-hand side, as factors under the integral sign, an even power of $\cos u$ and also a $\sin(\delta\cos u)$, consequently $f^{2n}(0) = 0$.

For the odd derived function, the law is best expressed as follows:—

$$(2n+3)f^{2n+1}(\delta) + \delta f^{2n+2}(\delta) = (-1)^n \int_0^\epsilon \cos^{2n+1}u\cos(\delta\cos u)\,du,$$

whence $$(2n+3)f^{2n+1}(0) = (-1)^n \int_0^\epsilon \cos^{2n+1}u\,du.$$

Six terms in the expansion, *i.e.* proceeding to f^{xi}, were found to be sufficient for the range of fairly small δ's dealt with by this method.

The values of the integrals $\int_0^\epsilon \cos^{2n+1}u\,du$ were obtained by expressing the powers of $\cos u$ in terms of cosines of multiples of u and then integrating. The values so obtained were—

$$f^{\mathrm{i}}(0) = \tfrac{1}{3}\sin\epsilon,$$

$$f^{\mathrm{iii}}(0) = -\tfrac{1}{5}\left(\frac{\sin 3\epsilon}{12} + \frac{3\sin\epsilon}{4}\right),$$

$$f^{\mathrm{v}}(0) = \tfrac{1}{7}\left\{\frac{\sin 5\epsilon}{80} + \frac{5\sin 3\epsilon}{48} + \frac{5\sin\epsilon}{8}\right\},$$

$$f^{\mathrm{vii}}(0) = -\tfrac{1}{9}\left\{\frac{\sin 7\epsilon}{448} + \frac{7\sin 5\epsilon}{320} + \frac{7\sin 3\epsilon}{64} + \frac{35\sin\epsilon}{64}\right\}$$

$$f^{\mathrm{ix}}(0) = \tfrac{1}{11}\left\{\frac{\sin 9\epsilon}{2304}+\frac{9\sin 7\epsilon}{1792}+\frac{9\sin 5\epsilon}{320}+\frac{7\sin 3\epsilon}{64}+\frac{63\sin\epsilon}{128}\right\},$$

$$f^{\mathrm{xi}}(0) = -\tfrac{1}{13}\left\{\frac{\sin 11\epsilon}{11264}+\frac{11\sin 9\epsilon}{9216}+\frac{55\sin 7\epsilon}{7168}+\frac{33\sin 5\epsilon}{1024}+\frac{55\sin 3\epsilon}{512}+\frac{231\sin\epsilon}{512}\right\}.$$

In using this method it was found most convenient to calculate the general term $\frac{\delta^n}{n!}f^n(0)$ as the product of δ^n and $\frac{1}{n!}f^n(0)$, so that on one sheet were calculated the values of the latter function for values of ϵ by intervals of 5° from 0 to $\frac{1}{2}\pi$, giving coefficients which, when multiplied by the respective values of δ^n and summed, provided the values of I.

The calculations were rendered less tedious by the use of a Brunsviga calculator.

Table I.*—Calculation of $\frac{1}{n!}f^n(0)$.

	5°.	10°.	15°.
$\sin\epsilon$	0·0871557	0·1736482	0·2588190
$\sin 3\epsilon$	0·2588190	0·5000000	0·7071068
$\sin 5\epsilon$	0·4226183	0·7660444	0·9659258
$\sin 7\epsilon$	0·5735764	0·9396926	0·9659258
$\sin 9\epsilon$	0·7071068	1·0000000	0·7071068
$\sin 11\epsilon$	0·8191520	0·9396926	0·2588190
$\frac{1}{3}\sin\epsilon$	0·0290519	0·0578827	0·0862730
$\frac{\sin 3\epsilon}{12}$	0·0215683	0·0416667	0·0589256
$\frac{3\sin\epsilon}{4}$	0·0653668	0·1302362	0·1941143
sum	0·0869351	0·1719029	0·2530399
$\frac{1}{30}$ sum	0·00289784	0·005730097	0·008434663
$\frac{\sin 5\epsilon}{80}$	0·00528273	0·00957556	0·01207407
$\frac{5\sin 3\epsilon}{48}$	0·02696031	0·05208333	0·07365696
$\frac{5\sin\epsilon}{8}$	0·05447231	0·10853013	0·16176188
sum	0·08671535	0·17018902	0·24749291
$\frac{1}{840}$ sum	0·0001032326	0·0002026060	0·00029463442

* This table and those on pp. 307 and 308 were calculated to more figures than are requisite for the final results, as, *a priori*, the degree of approximation required could not be determined.

Table I.—*continued.*

	5°.	10°.	15°.
$\frac{\sin 7\epsilon}{448}$	0·00128030	0·00209753	0·00215608
$\frac{7\sin 5\epsilon}{320}$	0·00924478	0·01675722	0·02112963
$\frac{7\sin 3\epsilon}{64}$	0·02830833	0·05468750	0·07733981
$\frac{35\sin \epsilon}{64}$	0·04766327	0·09496386	0·14154164
sum	0·08649668	0·16850611	0·24216716
$\frac{\text{sum}}{45360}$	$0\cdot01906893\times10^{-4}$	$0\cdot03714861\times10^{-4}$	$0\cdot05338782\times10^{-4}$
$\frac{\sin 9\epsilon}{2304}$	0·00030690	0·00043403	0·00030690
$\frac{9\sin 7\epsilon}{1792}$	0·00288069	0·00471944	0·00485119
$\frac{9\sin 5\epsilon}{320}$	0·01188614	0·02154500	0·02716666
$\frac{7\sin 3\epsilon}{64}$	0·02830833	0·05468750	0·07733981
$\frac{63\sin \epsilon}{128}$	0·04289695	0·08546747	0·12738748
sum	0·08627901	0·16685344	0·23705204
$\frac{\text{sum}}{3991680}$	$0\cdot02161471\times10^{-6}$	$0\cdot04180030\times10^{-6}$	$0\cdot05938653\times10^{-6}$
$\frac{\sin 11\epsilon}{11264}$	0·00007272	0·00008342	0·00002298
$\frac{11\sin 9\epsilon}{9216}$	0·00084399	0·00119358	0·00084399
$\frac{55\sin 7\epsilon}{7168}$	0·00440105	0·00721025	0·00741054
$\frac{33\sin 5\epsilon}{1024}$	0·01361954	0·02468698	0·03112847
$\frac{55\sin 3\epsilon}{512}$	0·02780282	0·05371094	0·07595874
$\frac{231\sin \epsilon}{512}$	0·03932220	0·07834518	0·11677185
sum	0·08606232	0·16523035	0·23213657
$\frac{\text{sum}}{518918400}$	$0\cdot16584942\times10^{-9}$	$0\cdot31841297\times10^{-9}$	$0\cdot44734696\times10^{-9}$

Table II.—Calculation of I.

		5°.	10°.	15°.
$\delta = 2\cdot0-$				
δ	2	0·0581038	0·1157654	0·1725460
δ^3	8	−0·0231827	−0·0458408	−0·0674773
δ^5	32	0·0033034	0·0064834	0·0094283
δ^7	128	−0·0002441	−0·0004755	−0·0006834
δ^9	512	0·0000111	0·0000214	0·0000304
		0·0379915	0·0759539	0·1138440
$\delta = 2\cdot4-$				
δ	2·4	0·0697246	0·1389185	0·2070552
δ^3	13·824	−0·0400597	−0·0792129	−0·1166003
δ^5	79·6264	0·0082200	0·0161328	0·0234606
δ^7	458·647142	−0·0008746	−0·0017038	−0·0024486
δ^9	2641·807538	0·0000571	0·0001104	0·0001569
δ^{11}	15216·81137	−0·0000025	−0·0000048	−0·0000068
		0·0370649	0·0742402	0·1116165
$\delta = 2\cdot7-$				
δ	2·7	0·0781401	0·1562832	0·2329371
δ^3	19·683	−0·0570382	−0·1127855	−0·1660195
δ^5	143·48907	0·0148127	0·0290717	0·0422768
δ^7	1046·0353	−0·0019947	−0·0038859	−0·0055846
δ^9	7625·5973	0·0001648	0·0003187	0·0004529
δ^{11}	55590·6043	−0·0000092	−0·0000177	−0·0000249
		0·0343755	0·0689845	0·1040378

5. Evaluation by mechanical integration. For the values of δ between 3·83 and 16·47 mechanical integration was employed. Here it was found desirable to alter the form of the expression to be integrated, so that it would be less cumbersome in the work of computing the points on the curve before plotting.

Putting $z = \frac{1}{v}\left(\frac{\sin v}{v} - \cos v\right)$, then $I = \int_0^\epsilon z\,du$;

and if we plot z against u, the area up to any value ϵ of u will be the value of I for that ϵ.

Put $v = \delta \cos u = \tan\phi$,

then $z = \frac{1}{v}\left(\frac{\sin v}{\tan\phi} - \cos v\right) = \frac{\sin v\cos\phi - \cos v\sin\phi}{v\sin\phi}$;

therefore $z = \frac{\sin(v-\phi)}{v\sin\phi}$,

and this is a form eminently suited to logarithmic calculation.

The work was arranged in parallel columns, each column for one value of u and each sheet containing all the work for one value of δ. For the preliminary calculations, values of u were taken at intervals of 5°, the values of z so obtained were plotted on squared paper, and the maxima and minima (which will be separately discussed) inserted. From this graph it was evident what further points were required in order to draw the curve of z accurately. This rough plotting on squared paper served as a very useful check against errors in the work of calculation. The arrangement is shown in Table III.

The positions of the maxima and minima were calculated by a different method.

Table III.—Calculation of z.

$\delta = 11{\cdot}61986$.

	0°.	5°.	10°.	15°.	Max.
$\log \delta$	1·0652009	1·0652009	1·0652009	1·0652009	1·0652009
$\log \cos u$	—	9·9983442	9·9933515	9·9849438	9·2531911
$\log v = \log \tan \phi$	—	1·0635451	1·0585524	1·0501447	0·3183920
ϕ	85° 4′ 52″·6	85° 3′ 45″·3	85° 0′ 20″·8	84° 54′ 31″·2	
v in radians	11·619860	11·575616	11·443330	11·223922	
v in degrees	665° 46′ 8″·2	663° 14′ 2″·2	655° 39′ 16″·1	643° 5′ 0″·1	
$v - \phi$	580° 41′ 15″·6	578° 10′ 16″·9	570° 38′ 55″·3	558° 10′ 28″·9	
$\log \sin \phi$	9·9983977	9·9983855	9·9983480	9·9982831	
$\log \left(\frac{1}{\sin \phi}\right)$	0·0016023	0·0016145	0·0016520	0·0017169	$u = 79°{\cdot}680$
$\log \left(\frac{1}{v}\right)$	8·9347991	8·9364549	8·9414476	8·9498553	
$\log \sin (v-\phi)$*	9·8142034n	9·7909994n	9·7073766n	9·4940367n	
$\log z$	8·7506048n	8·7290688n	8·6504762n	8·4456089n	
z	−0·056312	−0·053588	−0·044717	−0·027900	

* n in this table denotes that the numerical quantity of which the logarithm is given occurs with a negative sign.

Since $$z = \frac{1}{v}\left(\frac{\sin v}{v} - \cos v\right) \quad \text{and} \quad v = \delta \cos u,$$

then $$\frac{dz}{du} = \frac{dz}{dv} \cdot \frac{dv}{du} = \frac{dz}{dv} \cdot (-\delta \sin u).$$

Hence, for any value of δ, not zero, u not being zero, dz/du and dz/dv have their zero values simultaneously; consequently, instead of considering $dz/du = 0$, we may take $dz/dv = 0$. We have then—

$$0 = \frac{dz}{dv} = -\frac{2}{v^3} \sin v + \frac{2}{v^2} \cos v + \frac{1}{v} \sin v,$$

or $$\sin v\left(\frac{2}{v^3}-\frac{1}{v}\right)=\frac{2\cos v}{v^2}, \quad i.e. \quad \tan v=\frac{2v}{2-v^2},$$

and the roots of this equation give the values of v, and therefore of u, for which z is a maximum or minimum.

The roots were found by successive approximation.

Put $$v = v_0+\epsilon,$$

then $$\tan(v_0+\epsilon)=\frac{2(v_0+\epsilon)}{2-(v_0+\epsilon)^2}.$$

Now expand the left-hand side by Taylor's theorem and the right by the binomial, neglecting second and higher powers of ϵ.

Then

$$\tan v_0+\frac{\epsilon}{\cos^2 v_0}=\frac{2(v_0+\epsilon)}{2-{v_0}^2-2v_0\epsilon}=\frac{2v_0}{2-{v_0}^2}+\epsilon\left\{\frac{2}{2-{v_0}^2}+\frac{4{v_0}^2}{(2-{v_0}^2)^2}\right\};$$

Therefore

$$\epsilon=\frac{\tan v_0-\frac{2v_0}{2-{v_0}^2}}{\frac{2}{2-{v_0}^2}+\frac{4{v_0}^2}{(2-{v_0}^2)^2}-\sec^2 v_0}=\frac{2-{v_0}^2}{{v_0}^2}\left\{\tan v_0-\frac{2v_0}{2-{v_0}^2}\right\}$$

$$=\frac{2}{v_0}\left(1-\frac{2v_0}{2-{v_0}^2}\cot v_0\right).$$

This formula was not very often required, as is easily seen from the following considerations. Counting the maxima and minima from $u=\frac{1}{2}\pi$ backwards to $u=0$, there is only a limited number of them for any given value of δ; moreover, these maxima and minima occur with precisely the same values of v and z, when δ takes up a new value, the only change with regard to them being that u changes its value in accordance with $v=\delta\cos u$. The values of the maxima and minima may be calculated by the same method as the other values of z, or more shortly as follows:—

$$\tan v=\frac{2v}{2-v^2};$$

therefore $$z=\frac{1}{v}\left(\frac{2}{\sqrt{(4+v^4)}}-\frac{2-v^2}{\sqrt{(4+v^4)}}\right)=\frac{v}{\sqrt{(4+v^4)}}.$$

All the data required for the plotting of the curves of z for the different values of δ being now obtained, the curves were plotted on large, thin, smooth-surfaced* cards in rectangular co-ordinates by means of a Coradi co-ordinatograph, and the curves drawn in with the weights and splines used in naval architecture. The integration was then performed by means of a large Coradi integraph, which draws the graph of the integrated function. The cards were again placed under the co-ordinatograph, and

* Because both co-ordinatograph and integraph work best on such cards.

the ordinates ruled for successive values of ϵ, increasing by steps of 2°. The photograph of such a card is shown on a much reduced scale in Diagram 1.

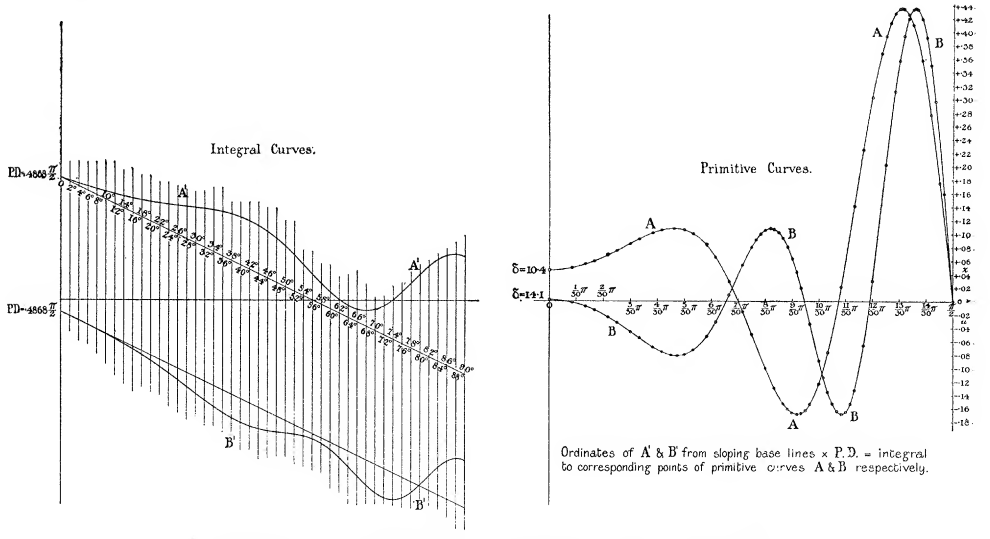

DIAGRAM 1.—Mechanical Integration of the I-Integral.
(Reduced to 1/6 linear of original drawing.)

The values of δ first taken were those giving the maxima and minima of the ring system of the circular aperture, and afterwards a sufficient number of intermediate values were taken to give an accurate curve when H was plotted against δ. The values of the ordinates of the integrated curve were scaled off and tabulated. For the angles 10°, 20° . . . 80°, 90° and $\delta = 3{\cdot}83$ . . . the values of I were obtained by both methods, and these values were compared. The values are given in Table IV.

Table IV.

	10°.	20°.	30°.	40°.	50°.	60°.	70°.	80°.	90°.
Direct calculation	0·0283	0·0617	0·1046	0·1603	0·2285	0·3039	0·3749	0·4266	0·4455
By mechanical integration	0·0283	0·0616	0·1046	0·1603	0·2290	0·3044	0·3752	0·4272	0·4460

These show a maximum difference of 1 in 457, or about 2 per mille. The greater the value of δ, however, the greater the inaccuracy of the mechanical integration, but the increase is slow; but, on the other hand, we have also a less accurate result from the less convergent series.

6. The evaluation and representation of H.

The value of H was obtained by combining the two parts C and S. Putting $\pi\gamma^2 = 2$, we have $C = J_1(\delta) \times \frac{2}{\delta}$, and $S = \frac{4}{\pi}I$. This part of the work was also carried out in tabular form, one sheet being used for each value of δ. The values of H had now been obtained for a meshwork of points, but the bare figures did not help one to realise the appearance of the diffraction image. Representation by means of a model was unfortunately out of the question, as the ratio of the intensities in different regions of the figure is too great. It was found far more useful to construct a diagram showing contour lines or lines of equal light intensity. In order to do this, interpolation curves had to be drawn for every value of ϵ, plotting H against δ. It was found necessary to draw each curve in several overlapping sections, using different

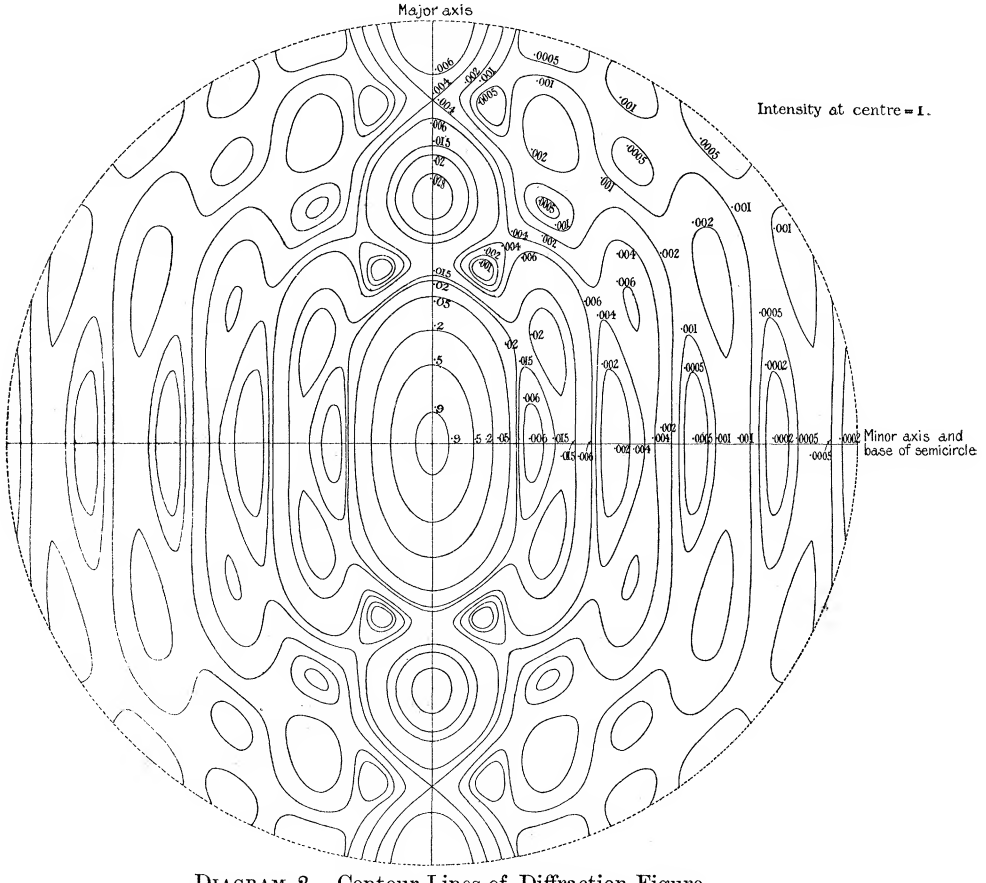

DIAGRAM 2.—Contour Lines of Diffraction Figure.

(Reduced to $\frac{1}{4{\cdot}5}$ linear of original drawing.)

scales for each, in consequence of the large range in value of H. These curves were drawn upon squared paper, which for this purpose was found sufficiently accurate. The values of δ, at which H took up any desired value, were then tabulated for the intervals of ϵ adopted, and from this table the contour diagram was constructed. This Diagram (2) was plotted on a large scale, and then photographically reduced. The central intensity being unity, the values of H used were 0·9, 0·5, 0·2, 0·05, 0·02, 0·015, 0·006, 0·004, 0·002, 0·001, 0·0005, and 0·0002. The contour diagram shows all the features seen when the diffraction image is examined visually, as is evident on comparison with the photograph taken for that purpose.

7. Having obtained the diffraction figure up to a distance of $\delta = 16{\cdot}47$, two questions at once presented themselves: (*a*) what is the accuracy of the result, and (*b*) is it desirable to extend our knowledge any further. Dealing with the latter question first, it certainly does seem desirable to trace the fluctuations of light along the bright ray which forms the major axis of the figure; and this, being carried out by direct calculation, will serve as a test of the accuracy of the mechanical integration at the part of the range where the accuracy so obtainable is smallest. The formulæ hitherto used will not serve when δ is, as now, large. Bruns gives as an alternative expression for S,

$$S = \frac{2\gamma^2}{\delta \sin \alpha}\left[\frac{4}{1.3} J_2(\delta) \sin 2\alpha + \frac{8}{3.5} J_4(\delta) \sin 4\alpha + \frac{12}{5.7} J_6(\delta) \sin 6\alpha + \ldots\right],$$

where $$\alpha = \epsilon - \tfrac{1}{2}\pi.$$

Now, for the major axis of the figure $\alpha = 0$.

Hence we have

$$S = \frac{2\gamma^2}{\delta}\left[\frac{4.2}{1.3} J_2(\delta) + \frac{8.4}{3.5} J_4(\delta) + \frac{12.6}{5.7} J_6(\delta) + \ldots\right].$$

Putting in the value of γ^2, and taking a factor 8 out of the bracket, we have

$$S = \frac{32}{\pi\delta} \sum_1^\infty \frac{n^2 J_{2n}(\delta)}{4n^2 - 1},$$

which may also be written

$$S = \frac{8}{\pi\delta}\left\{\sum_1^\infty J_{2n}(\delta) + \sum_1^\infty \frac{J_{2n}\delta}{4n^2 - 1}\right\},$$

or

$$S = \frac{8}{\pi\delta}\left\{\frac{1 - J_0(\delta)}{2} + \sum^\infty \frac{J_{2n}(\delta)}{4n^2 - 1}\right\}.$$

The values of H were then calculated for $\delta = 10, 14, 15, \ldots 24$ and plotted; intermediate values of H required for splining were obtained by interpolation, using a parabola of the third order, this being far quicker than interpolating for each $J_{2n}(\delta)$ required. This method served up to $\delta = 24$, at which argument the tables of J's at present end. The values of H for $\epsilon = \frac{1}{2}\pi$ were then tabulated and the graph of H against $\delta\,(\epsilon = \frac{1}{2}\pi)$ drawn.

The value of H was obtained by both methods in four cases and the results are given in Table V. It is at once evident that the mechanical integration gives accurate results, the maximum error barely exceeding one unit in the fourth place of decimals.

Table V.

δ.	10·0.	14·0.	15·0.	16·0.
Mechanical integration.....	0·0318	0·0049	0·0085	0·0104
Direct calculation	0·03189	0·00493	0·00850	0·01056

The above method, as I have said, was available up to $\delta = 24$, beyond which the J's are not yet tabulated. As this range does not carry us beyond the third bright spot, and it was desired to go further than this, another method was necessary. After several futile attempts, such a method was found and has proved itself very useful. It would, of course, have been possible to have computed all the J's required (a very large number), but the labour would have been excessive and the following method was adopted to lessen the work:—

$$\sin(x\sin\phi) = 2\{J_1(x)\sin\phi + J_3(x)\sin 3\phi + \ldots\},$$

$$\int \sin(x\sin\phi)\,d\phi = -2\{J_1(x)\cos\phi + \tfrac{1}{3}J_3(x)\cos 3\phi + \ldots\},$$

$$\int_0^{\frac{1}{2}\pi} \sin(x\sin\phi)\,d\phi = 2\{J_1(x) + \tfrac{1}{3}J_3(x) + \tfrac{1}{5}J_5(x) + \ldots\}.$$

Differentiate both sides with regard to x—

$$\int_0^{\frac{1}{2}\pi} \cos(x\sin\phi)\sin\phi\,d\phi = 2\{J_1'(x) + \tfrac{1}{3}J_3'(x) + \tfrac{1}{5}J_5'(x) + \ldots\},$$

but $$J_n'(x) = \tfrac{1}{2}\{J_{n-1}(x) - J_{n+1}(x)\},$$

therefore

$$\begin{aligned}\int_0^{\frac{1}{2}\pi} \cos(x\sin\phi)\,d(\cos\phi) &= \{-J_0(x) - \tfrac{1}{3}J_2(x) - \tfrac{1}{5}J_4(x) - \tfrac{1}{7}J_6(x) - \ldots \\ &\qquad + J_2(x) + \tfrac{1}{3}J_4(x) + \tfrac{1}{5}J_6(x) + \ldots\} \\ &= -J_0(x) + (1-\tfrac{1}{3})J_2(x) + (\tfrac{1}{3}-\tfrac{1}{5})J_4(x) + \ldots \\ &\qquad + \left(\frac{1}{2n-1} - \frac{1}{2n+1}\right)J_{2n}(x) + \ldots \\ &= -J_0(x) + \sum_1^\infty \frac{2J_{2n}(x)}{4n^2-1}.\end{aligned}$$

Therefore $$\sum_1^\infty \frac{J_{2n}(x)}{4n^2-1} = \tfrac{1}{2}J_0(x) + \tfrac{1}{2}\int_0^{\frac{1}{2}\pi} \cos(x\sin\phi)\,d(\cos\phi).$$

Substituting this value in

$$S = \frac{8}{\pi\delta}\left\{\frac{1-J_0(\delta)}{2}+\sum_1^\infty \frac{J_{2n}(\delta)}{4n^2-1}\right\},$$

we have

$$S = \frac{8}{\pi\delta}\left\{\tfrac{1}{2}+\tfrac{1}{2}\int_0^{\frac{1}{2}\pi}\cos(\delta\sin\phi)\,d(\cos\phi)\right\};$$

or, putting $z = \cos\phi$,

$$S = \frac{4}{\pi\delta}\left\{1-\int_0^1 \cos(\delta\sqrt{(1-z^2)}\,dz)\right\}.$$

The determination of S resolves itself, therefore, into the evaluation of this integral. The method adopted may be called a semi-graphic one and is identical with that used independently by J. H. Shaxby and described by him in a paper read before the Royal Society on April 22, 1909.

The method had been found, tested and definitely adopted for this work at the end of the Lent term, and before I was aware by Mr. Shaxby's paper that he also had discovered its advantages. The method depends on the property possessed by this class of curves that, after cutting the axis a third time, the areas of all the other sections are almost identical with the areas of sine curves of the same altitude on the bases formed by the various points of intersection of the original curve with the axis. This is seen from the values given for $\delta = 33$ and $\delta = 40$ in Table VI.

Table VI.—Areas of Sections.

	$\delta = 33$.		$\delta = 40$.	
	Calculated.	Planimeter.	Calculated.	Planimeter.
1st partial section.....	—	0·0001	—	0·0873
1st complete section.....	0·2538	0·2113	0·1522	0·1469
2nd ,, ,, ...	0·1024	0·1016	0·0868	0·0862
3rd complete section.....	0·0717	0·0717	0·0638	0·0636
4th ,, ,, ...	0·0543	0·0545	0·0501	0·0501
5th ,, ,, ...	0·0423	0·0424	0·0405	0·0404
6th ,, ,, ...	0·0329	0·0329	0·0329	0·0331
7th ,, ,, ...	0·0250	0·0249	0·0268	0·0269
8th ,, ,, ...	0·0181	0·0181	0·0214	0·0216
9th ,, ,, ...	6·0118	0·0117	0·0165	0·0164
10th ,, ,, ...	0·0058	0·0059	0·0121	0·0120
11th ,, ,, ...	0·0007	0·0007	0·0080	0·0080
12th ,, ,, ...	—	—	0·0039	0·0036
13th ,, ,, ...	—	—	0·0005	0·0005

The horizontal line drawn through the above table marks where the curve cuts the axis for the third time. Beyond this point the calculated areas are practically identical with the planimetered areas of the curve.

The curve of $y = \cos \delta\sqrt{(1-z^2)}$ was therefore traced from $z = 0$ up to the point where it cut the axis for the *third* time and the area measured by a Coradi's Compensating Planimeter; the other points of intersection were calculated, the areas of sine curves on the bases so obtained computed and the whole area of the curve or value of the integral obtained by addition.

In dealing with graphs of this curve $y = \cos \delta (1-z^2)^{\frac{1}{2}}$, the usual practice of calculating ordinates for arbitrarily assigned abscissæ was reversed; the ordinates were arbitrarily fixed such that they would give equal increments of abscissa if the curve were a sine curve and the corresponding abscissæ were calculated for the actual curve; this method giving the points of intersection directly and also dividing the calculated points fairly evenly along the curve to be traced.

Accordingly a sufficient number of values of x were taken and the ordinates were $\cos x$.

Then z the abscissa of our actual curve was given by

$$z = \left\{1 - \left(\frac{2\pi n + x}{\delta}\right)^2\right\}^{\frac{1}{2}},$$

n being an integer and ranging from 0 upwards so long as z remains real.

Table VII.

	a.	*b.*	*c.*	*d.*
$2\pi n$	31·41593	31·41593	31·41593	31·41593
x	1·57080	1·39626	1·22173	1·04720
$2\pi n + x$	32·98673	32·81219	32·63766	32·46313
$\log (2\pi n + x)$	1·51834	1·51604	1·51372	1·51139
$\log \left(\frac{1}{\delta}\right)$	8·39794	8·39794	8·39794	8·39794
$\log \left(\frac{2\pi n + x}{\delta}\right)$	9·91628	9·91398	9·91166	9·90933
$2\log \left(\frac{2\pi n + x}{\delta}\right) = \log b$	9·83256	9·82796	9·82332	9·81866
$B = \log (1) - \log b$	0·16744	0·17204	0·17668	0·18134
A	9·67247	9·68670	9·70074	9·71453
$\log z^2 = \log b + A$	9·50503	9·51466	9·52406	9·53319
$\log z$	9·75251	9·75733	9·76203	9·76660
z	0·56560	0·57191	0·57814	0·58425

In the numerical work of computing z (shown in Table VII) use was made of the tables of "Additions- und Subtraktions-Logarithmen," given in Bremiker's five-figure logarithmic tables, which are specially suited to the type of formula in question. The specimen in Table VII is written out at full length, but in the actual work the starting point was of course $\log (2\pi n + x)$ and the line B was omitted.

The small letters over the columns indicate to which of the arbitrarily fixed ordinates the abscissa z corresponds.

The curve was, as before, plotted on cards with the co-ordinatograph and drawn in by the help of a spline. The complete curve for $\delta = 40$ is reproduced in Diagram 3.

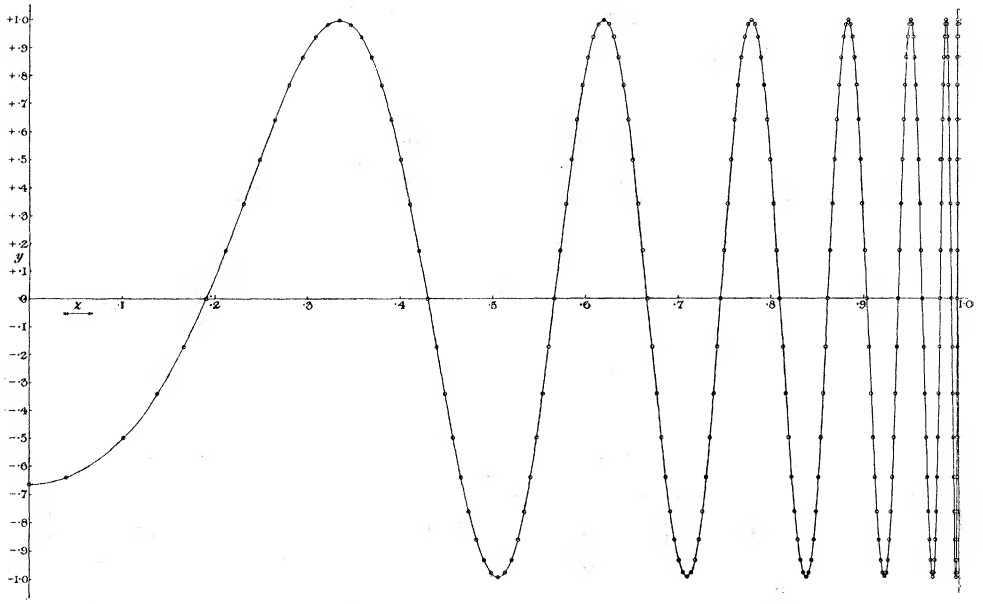

DIAGRAM 3.—Graph of $y = \cos \delta (1 - z^2)^{\frac{1}{2}}$ for $\delta = 40$, to show approach of areas to those of sine curve. (Reduced to 1/4 linear of original drawing.)

The planimetered areas, when added to the residual areas calculated by fitting halves of sine curves, gave the required integral, and consequently S. The value of C was found from the values of $J_1(\delta)$ as before; but these could not now be taken from tables of Bessel functions, and therefore were computed from the well-known semi-convergent series.* The accuracy of the values of H so obtained is very good indeed, as is shown by comparing

* Gray and Mathews, 'Treatise on Bessel Functions,' p. 40.

the value obtained by the above method and that by summation of J's for the case of $\delta = 24$, where the two methods link up—

By summation of J's	$H = 0{\cdot}003478$
By semi-graphic method	$H = 0{\cdot}003479$

This unusual accuracy is due to the fact that the integral evaluated is small and is subtracted from unity, thus decreasing the percentage error, which here is only 1/30 per cent.

The values of H have been tabulated for the cases of the two principal axes of the diffraction figure, $\epsilon = 0$ and $\epsilon = \frac{1}{2}\pi$, and from these have been drawn the curves of intensity of illumination along these axes (Diagram 4). Of course the intensity along the axis $\epsilon = 0$ is identical with the intensity along any radial line in the diffraction image of a circular aperture.

In the diagram the curve of intensity along the major axis of the diffraction figure is called A, and that for the minor axis B.

In the upper right-hand corner the curves are drawn together for the

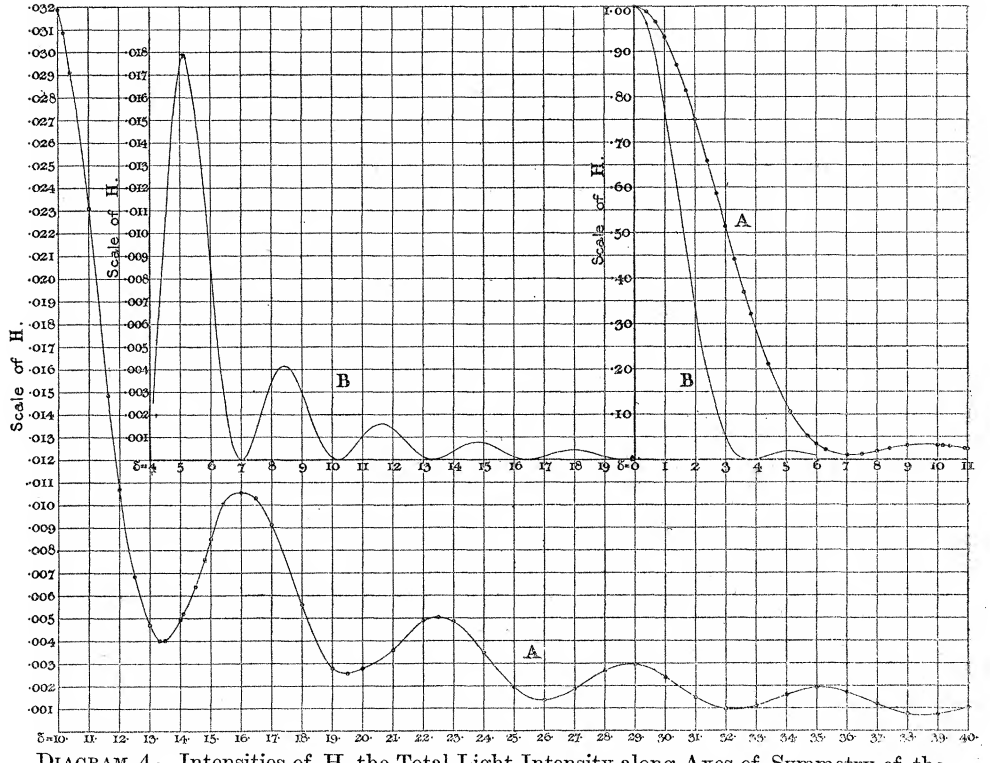

DIAGRAM 4.—Intensities of H, the Total Light Intensity along Axes of Symmetry of the Diffraction Figure. (Reduced to 1/5 linear of original.)

A, Major axis and axis of symmetry of semicircle.

B, Minor axis, perpendicular to axis of symmetry of semicircle.

central region of the image, the horizontal and vertical scales having as their respective units $\delta = 1$ and $H = 0{\cdot}05$. For the outer regions of the image, it was found best to draw A and B separately and on an enlarged vertical scale, the new unit being $H = 0{\cdot}001$, thus giving a magnification of 50, when compared with the central portion.

The curve of B is drawn on the enlarged scale from $\delta = 4$ to $\delta = 20$, and A from $\delta = 10$ to $\delta = 40$. It will be seen that A has minima but no zeros.

The curve B was not drawn beyond $\delta = 20$, as it is required only for comparison with A, and its last maximum shown is less than the last shown minimum of A. The values from which the curves have been drawn are given in Tables VIIIA and VIIIB for A and B respectively, and the methods by which the values were obtained are indicated.

Table VIIIA.—Values of H ($\epsilon = \frac{1}{2}\pi$).

δ.	H.	δ.	H.	δ.	H.
0·0	1·00000*	10·0	0·03189‡	20·0	0·00280‡
0·4	0·98887*		(0·0318)†	21·0	0·00359‡
0·7	0·96624*	10·1734	0·03087†	22·0	0·00490‡
1·0	0·93212*	10·4	0·02912†	22·5	(0·00504)‡
1·4	0·87059*	10·9	0·02828†	23·0	0·00485‡
1·7	0·81422*	11·0	(0·0231)†	24·0	0·00348‡
2·0	0·75092*	11·6199	0·01485†		0·00348§
2·4	0·65887*	12·0	(0·0107)†	25·0	0·00195§
2·7	0·58656*	12·5	0·00685†	26·0	0·00137§
3·0	0·51358*	13·0	(0·0047)†	27·0	0·00187§
3·3	0·44168*	13·3238	0·00401†	28·0	0·00268§
3·6	0·36920*	14·0	0·00493‡	29·0	0·00296§
3·8318	0·32160*		(0·0049)†	30·0	0·00238§
4·4	0·21091†	14·1	0·00519†	31·0	0·00149§
5·1356	0·10548†	14·7958	0·00760†	32·0	0·00097§
5·7	0·05182†	15·0	0·00850‡	33·0	0·00111§
6·0	0·03388†		(0·0085)†	34·0	0·00161§
6·3	0·02119†	15·4	0·01004†	35·0	0·00192§
6·7	0·01209†	15·9	0·01041†	36·0	0·00172§
7·0152	0·00986†	16·0	0·01056‡	37·0	0·00119§
7·5	0·01183†		(0·0104)†	38·0	0·00070§
8·0	0·01825†	16·470	0·01030†	39·0	0·00074§
8·4172	0·02401†	17·0	0·00912‡	40·0	0·00104§
9·0	0·03056†	18·0	0·00560‡		
9·5	0·03287†	19·0	0·00277‡		
		19·5	(0·00256)‡		

* Direct calculation (Taylor's theorem). † Mechanical integration.
‡ Direct calculation (J's). § Semi-graphic method.
( ) Interpolated.

Table VIIIB.—Values of H ($\epsilon = 0$).

δ.	H.	δ.	H.	δ.	H.
0·0	1·00000	7·5	0·00130	21·0	0·00027
0·4	0·96066	8·0	0·00344	22·0	0·00011
0·7	0·88356	8·4172	0·00416	23·0	0·00001
1·0	0·77458	9·0	0·00297	24·0	0·00016
1·4	0·59940	9·5	0·00115	25·0	0·00010
1·7	0·46203	10·1734	0·00000	26·0	0·00000
2·0	0·33261	10·4	0·00011	27·0	0·00010
2·4	0·18791	10·9	0·00087	28·0	0·00009
2·7	0·10700	11·6199	0·00161	29·0	0·00002
3·0	0·05109	12·5	0·00070	30·0	0·00006
3·3	0·01789	13·3238	0·00000	31·0	0·00007
3·6	0·00281	14·1	0·00045	32·0	0·00000
3·8318	0·00000	14·7959	0·00078	33·0	0·00004
4·4	0·00850	15·4	0·00054	34·0	0·00006
5·1356	0·01750	15·9	0·00019	35·0	0·00001
5·7	0·01293	16·470	0·00000	36·0	0·00002
6·0	0·00851	17·0	0·00013	37·0	0·00005
6·3	0·00436	18·0	0·00044	38·0	0·00001
6·7	0·00081	19·0	0·00012	39·0	0·00001
7·0152	0·00000	20·0	0·00005	40·0	0·00004

Values obtained by direct calculation only.

Method of Photographing the Diffraction Image.

8. Although Scheiner and Hirayama have already published a photograph of the semicircular aperture diffraction figure, it seemed best to procure an independent picture of the fringes for comparison. Apparatus in use in the Observatory was employed as far as possible, and the only part specially made for the purpose was the aperture plate, of which a sketch is shown in Diagram 5.

The base plate has a hole near the centre, into which, on the lower side, a chisel-shaped straight-edge is so fitted that the edge of the plane surface lies in a plane above the upper surface of the plate and parallel to it; the edge is visible in the diagram in the centre of the hole. Over the upper surface of the plate, and a little above it, a carrier, with a circular hole in its centre and pivoted at one end, is moved parallel to the surface of the plate by a micrometer screw pushing the free end. The carrier is kept in good contact with the screw by a spiral spring. Into the circular hole of the carrier, a number of small circular discs may be fitted and fixed by two screws with washers, which are not shown. These discs have each a conical hole bored in the centre, the lower circular edge of which is in contact with the straight-edge already described. The two edges are kept in contact by a spring underneath the cross-bar shown near the micrometer screw. Finally the micrometer screw is fitted with a divided drum reading against

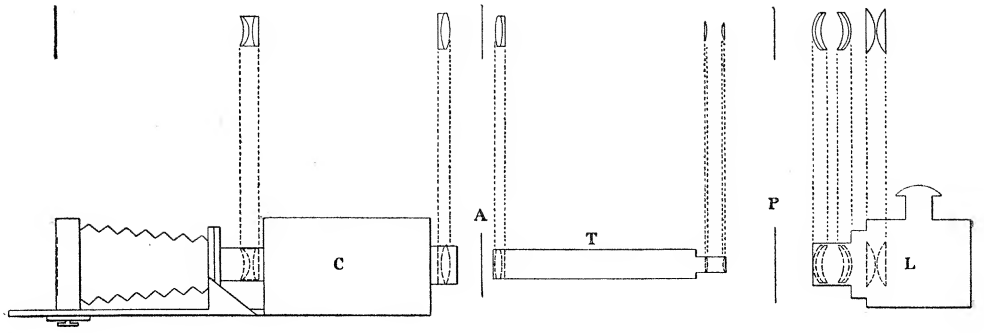

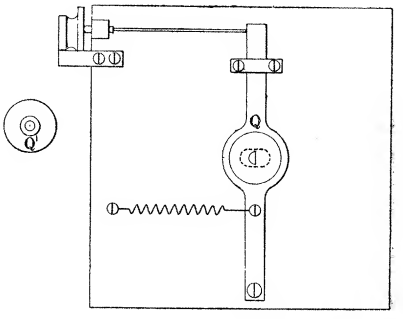

DIAGRAM 5.—Sketch of Apparatus employed.

a projecting scale. By this means the circular aperture is moved over the straight-edge until half of the circle is covered. The adjustment to the exact semicircle was made by means of a Hilger travelling microscope. This aperture was designed so that, after calibration of the micrometer screw, the diffraction fringes of any circular segment could be accurately found.

The remainder of the apparatus used and the general arrangement is shown in Diagram 5. The equivalent focus of the telephoto-camera was about 19 feet. In consequence of the optical peculiarities of such a system it was necessary, if this focus was to be retained, to have the point source of light at a great distance, which, unfortunately, could not be done A collimator was accordingly introduced; and, as the image of the pinhole source of light was magnified in the ratio of the foci of camera and collimator, a small image of the pinhole produced by an eye-piece was used, the only disadvantage being a largely increased exposure. The exposure required to obtain the photograph reproduced (Plate 3) was three hours. The greatest difficulty met with arose from the object-glass of the telescope having a number of waves of unequal refraction in the glass, and the parts so affected had to be most carefully avoided, as otherwise the diffraction image would have been adversely affected.

Comparison of Results.

9. We have now a contour diagram, two photographs and a diagram of the intensity along the principal axes of the diffraction image. How do these different results agree together ?

We have first to compare the results given for maxima and minima by the photographs and intensity curves. It was not possible to measure accurately the optical constants of the photographic apparatus used, so that the only available method of determining the reduction factor of my own photograph was to measure the dimensions along the minor axis—where the diffraction image is the same as that of a circular aperture. We have the following results :—

Table IX.—Major Axis.

	By intensity diagram.	By enlargement of own photograph.	By enlargement of Scheiner and Hirayama's plate.
1st min.	14·2	13·9	14·3
1st max.	19·4	19·4	19·9
2nd min.	26·8	—	26·8
2nd max.	32·0	31·8	32·6
3rd min.	38·9	—	—
3rd max.	44·9	44·2	45·1

These figures give the diameter of the image along the major axis bounded by the particular points of the image mentioned, and measured in terms of the adopted unit δ. The position and intensities of the maxima and minima along both axes are given below :—

Table X.

	Major axis.		Minor axis.	
	δ.	H.	δ.	H.
Centre	0·0	1·000	0·0	1·00000
1st min.	7·1	0·009	3·832	0·00000
1st max.	9·7	0·033	5·136	0·01750
2nd min.	13·4	0·00397	7·015	0·00000
2nd max.	16·0	0·01057	8·417	0·00416
3rd min.	19·45	0·00257	10·173	0·00000
3rd max.	22·45	0·00503	11·620	0·00161
4th min.	25·95	0·00137	13·324	0·00000
4th max.	28·85	0·00296	14·796	0·00078
5th min.	32·25	0·00095	16·470	0·00000
5th max.	35·15	0·00193	17·960	0·00043
6th min.	38·50	0·00068	19·616	0·00000

The values for the major axis were obtained from the intensity curve shown in Diagram 4, while those for the minor axis are, of course, the values for the diffraction image due to a circle. There is an interesting point about these values. In the case of the minor axis (or circle) each maximum lies nearer to the minimum of its own order than to that of the next higher order, but this tendency of the maxima decreases as the order increases, and ultimately vanishes. In the case of the major axis, the same tendency of the maxima is present; but it appears that the tendency, although becoming smaller, does so far less rapidly.

Turning now to the contour diagram (fig. 2), and comparing it with the photograph (Plate 3), the agreement is perfect; and while the photograph makes reference to the contour diagram easier, the contour diagram emphasises and extends the details of the photograph. From the contour diagram we see that the central spot is not really an ellipse, but only an approximation to one. Calling the five contour lines shown in the central spot A, B, C, D, E, counting from the centre outwards, we find, on measuring their diameters along the axes of the figure:—

Table XI.

	Major axis.	Minor axis.	Ratio.
A	2·436	1·296	1·88
B	6·114	3·234	1·90
C	8·814	4·720	1·87
D	11·446	6·020	1·90
E	12·686	6·550	1·94

We see that there is, on the whole, an increase in the ratio of the diameters, so that the shape of the central spot varies with the exposure when taking a photograph, and also with the intensity of the light when observed visually. The deviations from the steady increase in the ratio which are shown by B and C may be quite reasonably explained by the influence of the first bright ray, which should increase the ratio very slightly in the case of B, and of the first dark ray, which appears to decrease the ratio somewhat in the case of C. In connection with this, the way the contour line we have just called E is pulled out of shape is very significant.

10. General description of the diffraction image.

The image is, as has been already mentioned, symmetrical about two perpendicular axes. There is a central approximately oval spot, which is roughly a little less than twice as long as it is broad. This central spot is bisected along its major axis by a long bright ray, which fades away as it recedes from the centre. Around the spot and following its outline are a

Diffraction Fringes of Semicircular Aperture.

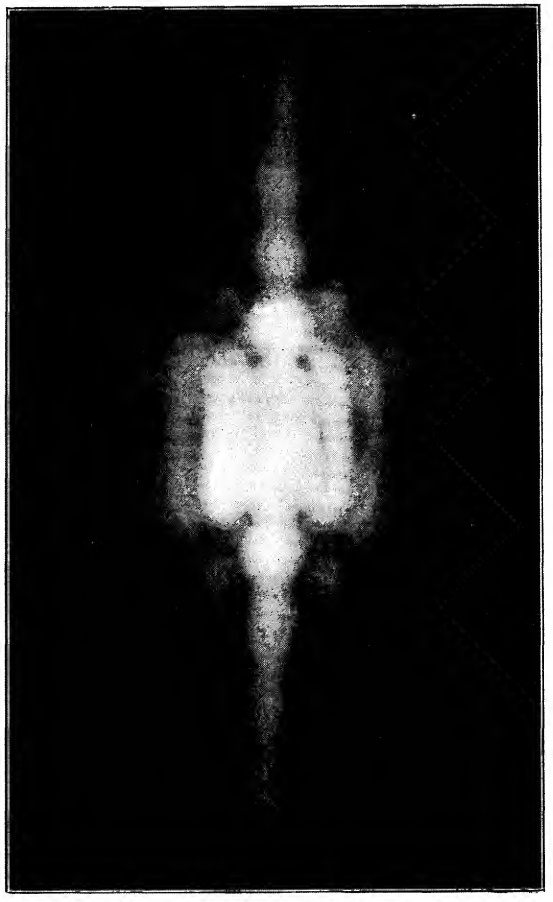

From photograph by author.]

(Enlarged.)

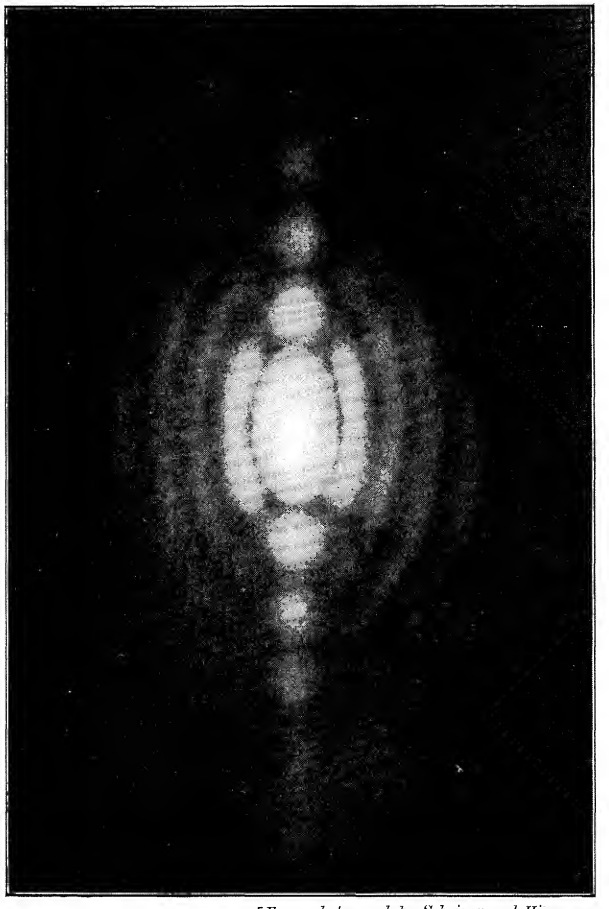

[*From photograph by Scheiner and Hirayama.*

(Enlarged.)

series of alternate dark and bright rings, which, at the minor axis, are identical with those of the diffraction image of a circular aperture, and, along the major axis, terminate at an angle in a series of bright spots. Further, these rings are crossed and modified by a series of alternate bright and dark rays of approximately hyperbolic shape, having the major axis of the figure for their geometric axis, which they cut at its maxima and minima, with the exception that the first one of the series passes through a point in the central bright spot. The whole diffraction image presents an exceedingly beautiful appearance, which is, unfortunately, only very inadequately represented by photography, but which is very easily studied with the double-star apparatus when monochromatic light is used and the star is examined in the equatorial through the heliometer lens.

Conclusions.

(i) The complex diffraction fringes due to a semicircular aperture have been for the first time theoretically determined, and actual measurements on the fringes themselves shown to be in close accordance with the calculated results. The absolute agreement of the computed contours with the photographs forms another item in the evidence, showing the old undulatory theory of light suffices to describe very accurately diffraction phenomena.

(ii) A problem which has attracted the attention of more than one astronomer and mathematician but had not yet been overcome, has been solved, and the exact nature of heliometer images numerically determined.

(iii) The solution of the problem has illustrated the limits to the practical utility of Bessel's functions; the mechanical integration of 24 indefinite and 17 definite integrals has indicated the manner in which graphical methods can be used to supplement numerical analysis, and has contributed to the solution of a physical and astronomical problem of considerable interest, which had hitherto proved unattainable by the usual methods of evaluation.

BIBLIOGRAPHY.

Bessel, 'Astronomische Untersuchungen,' Bd. I, 1841; 'Astronomische Nachrichten,' Bd. VIII, S. 411—426.

Bruns, "Über die Beugungsfiguren des Heliometer-Objectivs," 'Astron. Nachr.,' Bd. CIV, No. 2473.

H. Scheiner and S. Hirayama, "Photographische Aufnahmen Fraunhofer'scher Beugungsfiguren," 'Abhandl. Akad. Wiss. in Berlin,' 1894.

J. H. Shaxby, "On the Graphical Determination of Fresnel's Integrals," 'Roy. Soc. Proc.,' A, vol. 82, No. A 555.

Gray and Mathews, 'Treatise on Bessel Functions and their Application to Physics,' London, 1895.

Diffraction Fringes of Semicircular Aperture.

From photograph by author.]

(Enlarged.)

[*From photograph by Schemer and Hirayama*

(Enlarged.)